Published online 12 May 2022 *Nucleic Acids Research, 2022, Vol. 50, Web Server issue* ***W651–W656***
https://doi.org/10.1093/nar/gkac365

RING 3.0: fast generation of probabilistic residue interaction networks from structural ensembles

Damiano Clementel†, Alessio Del Conte†, Alexander Miguel Monzon, Giorgia F. Camagni, Giovanni Minervini, Damiano Piovesan and Silvio C.E. Tosatto*

Department of Biomedical Sciences, University of Padova, Padova 35131, Italy

Received March 23, 2022; Revised April 15, 2022; Editorial Decision April 21, 2022; Accepted April 30, 2022

ABSTRACT

Residue interaction networks (RINs) are used to represent residue contacts in protein structures. Thanks to the advances in network theory, RINs have been proved effective as an alternative to coordinate data in the analysis of complex systems. The RING server calculates high quality and reliable non-covalent molecular interactions based on geometrical parameters. Here, we present the new RING 3.0 version extending the previous functionality in several ways. The underlying software library has been re-engineered to improve speed by an order of magnitude. RING now also supports the mmCIF format and provides typed interactions for the entire PDB chemical component dictionary, including nucleic acids. Moreover, RING now employs probabilistic graphs, where multiple conformations (e.g. NMR or molecular dynamics ensembles) are mapped as weighted edges, opening up new ways to analyze structural data. The web interface has been expanded to include a simultaneous view of the RIN alongside a structure viewer, with both synchronized and clickable. Contact evolution across models (or time) is displayed as a heatmap and can help in the discovery of correlating interaction patterns. The web server, together with an extensive help and tutorial, is available from URL: https://ring.biocomputingup.it/.

GRAPHICAL ABSTRACT

INTRODUCTION

Proteins are large macromolecules interacting with a variety of different molecules to perform their functions in the cell. Non-covalent interactions stabilize the protein structure and govern its folding process (1). While the energy contribution of a single interaction is minimal, non-covalent interactions are responsible for supra-molecular binding and in essence provide the means for molecular communication (2). Whereas protein structure traditionally describes the shape of the protein itself, network theory can be used to focus on its interactions. Residue interaction networks (RINs), sometimes also known as protein structure networks (PSNs), consider amino acids as nodes and contacts as edges (3). Contacts are usually defined based on distance and additional parameters such as physico-chemical properties and geometrical constraints allowing to refine the network and characterize the type of interaction (4). Over the years, several methods have been developed to tackle this problem (5–10). For a recent review see (11). Our contribution to the field has been the Residue Interaction Network Generator (RING) software (12,13).

The field of RIN analysis has matured from proof of principle of the applicability of network parameters in static structures (14–17) to cover a variety of more specific applications. The RING output (12) has been successfully applied to study the effects of mutations, distinguishing different classes on the same protein (18), as well as to describe the interactions between globular domains and their intrinsically disordered binding partners (19). The accurate physico-chemical representation of non-covalent interactions offered by RING has been used to determine specific interactions (e.g. π–π stacks) in novel Cryo-EM structures (20,21). Protein–protein interactions such as the SARS-CoV2 with the ACE2 receptor (22) and photosystem II (23) as well as protein–nucleotide interactions in histones (24) have also been studied.

Describing the dynamics and allostery inherent in proteins (25) in the cellular environment with molecular dynamics (MD) simulations has become increasingly important for RIN analysis (11). The availability of longer MD

*To whom correspondence should be addressed. Tel: +39 049 827 6269; Fax: +39 049 827 6260; Email: silvio.tosatto@unipd.it
†The authors wish it to be known that, in their opinion, the first two authors should be regarded as joint First Authors.

simulations is posing new challenges, where it is necessary to extract meaningful conformational changes from a large number of structural snapshots. RING has been successfully used on single MD snapshots to estimate the enzyme activity-stability tradeoffs (26) as well as to study different conformations in human protein disulfide isomerase (27). Here, we present the new RING 3.0 version of the web server designed directly for MD experiments and multi-state structures. RING now generates probabilistic networks taking into consideration the frequency of connectivity across states (or snapshots). In addition, the software is about ten times faster, scaling linearly with protein size. RING 3.0 can process mmCIF files natively and handle the all hetero groups (e.g. modified residues) defined by the ww-PDB consortium. The web server has been completely re-implemented and visualizes the RIN graph alongside the protein structure. While anonymous usage of RING 3.0 is always permitted, interested users can choose to recover previous sessions via a private dashboard.

MATERIALS AND METHODS

The RING web server generates residue interaction networks with edges representing different physico-chemical types based on user input and displays the results via web. The basic workflow is similar to the previous RING version (12). In the following, we will explain the main changes introduced since the previous version of the server.

RING calculation

The RING calculation is based on typed interactions derived from physico-chemical parameters and geometrical constraints. Briefly put, all atom pairs from non-consecutive residues in the structure are scanned using a set of type-specific geometric cutoffs (i.e. distances and, where necessary, angles). The generated network thus represents non-covalent interactions between residues, providing a simplified and more abstract description of the structure. As in the previous version, RING interaction types are hydrogen bonds, disulfide bridges, ionic, Van der Waals, π–cation and π–π interactions. A detailed description of how they are defined is provided in (12) as well as through the RING website.

The RING executable has been improved by re-engineering the C++ Victor library (28), which provides basic input/output and efficient data structures for biological macromolecules. Inclusion of the CIFPARSE-OBJ library (https://www.iucr.org/resources/cif/software/cifparse-obj/) allows the processing of mmCIF files., enabling RING to handle very large structures with over 100 000 atoms. The inclusion of the chemical component dictionary (29) also improves handling of non-amino acid structures such as typed interactions for nucleic acids. Execution time for RING has been significantly improved by replacing the brute force approach of pairwise distance comparisons between all atoms in the structure with two heuristics for chains and amino acids. Contacts between different chains are only searched when the bounding boxes of the two chains overlap, i.e. the minimum and maximum values of their coordinates are in the same range. To reduce the number of comparisons further, the distance between carbon alpha pairs is calculated. Only for amino acid pairs where this value is below an empirical threshold are all atoms checked for possible typed interactions. The empirical distance threshold was estimated from the maximum distance between long side chains pointing towards each other plus the largest distance cutoff for an interaction. The chain heuristic ensures that RING 3.0 execution time remains roughly linear for large structures with many chains such as the ribosome. The amino acid heuristic reduces the execution time approximately by a factor of ten. For example, RING computation for the large RNA polymerase-Gfh1 complex (PDB code: 3AOH) containing 74 250 atoms is reduced from 1219 to just 22 s in the new version. Very large structures such as Virus-like particle of bacteriophage AC (PDB code: 6yf7) with 231 390 (computed in 33 s) can be handled by RING 3.0 thanks to the mmCIF format.

These improvements allow RING to process conformational ensembles such as multiple models in NMR structures and MD snapshots. The calculation scales linearly with the number of conformations, e.g. the structural ensemble of dihydrofolate reductase with 1548 atoms and 250 models (PDB code: 4P3R) takes less than 30 seconds. In these cases RING generates a probabilistic network, where edges have an associated weight (range: 0,..,1) representing the frequency in which the interaction was present in the conformational ensemble. The resulting network allows distinguishing stable from variable contacts in the conformational ensemble which can be used to pinpoint conformational changes. RING produces conformational dependent contact maps where contacts for each residue are separated by type and shown on a per-model basis (see Figure 1 for an example).

In addition to direct visualization on the web, the RING output can be downloaded in text format for nodes and edges as well as JSON format for use with Cytoscape (30) via the RINalyzer (17) and StructureViz (31) plugins.

Server implementation

The RING web server back-end is responsible for scheduling the execution of the RING software and managing authentication when requested. The back-end itself is based on the Django REST framework (URL: https://www.django-rest-framework.org/), which allows to create endpoints following the REST (REpresentational State Transfer) paradigm using the most commonly used web standards and data-interchange formats, such as HTML and JSON. Moreover, it improves maintenance by automatically implementing administration panels, database migrations and authentication. Users can either use the RING server anonymously or after authentication. The latter allows interested users access to a personal dashboard with all previous instances of RING execution. Authentication is based on the OAuth 2.0 protocol (URL: https://oauth.net/2/) and is available for all ORCID (URL: https://orcid.org/) and Google (URL: https://www.google.com/) users without additional registration. The back-end also allows programmatic access via the REST API.

The RING web interface is responsible for communicating with the back-end, rendering the network, load-

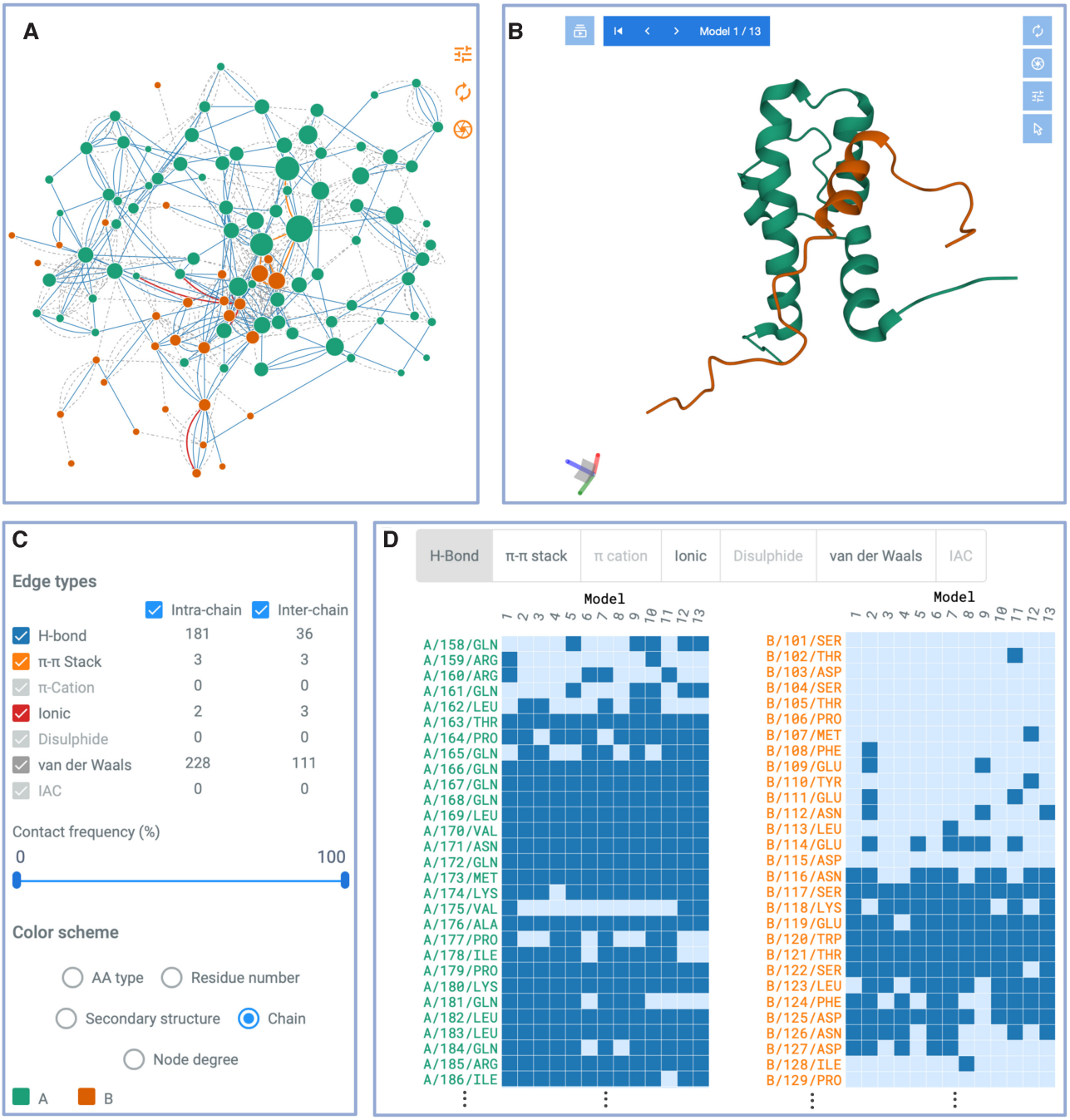

Figure 1. Main components of the RING web-server interface. The structure used for the example is an NMR ensemble complex (PDB code: 2LPB) of the mediator coactivator domain 1 of Gal11/med15 (Chain A, green) bound to the central activation domain of Gcn4 (Chain B, orange). (**A**) Interactive RIN with nodes colored by chain and edges by contact type. (**B**) Interactive protein structure viewer. Notice that the RIN and structure viewers are connected. Clicking on a residue in one panel will also highlight it in the other. (**C**) Control panel listing the intra- and inter-chain contacts grouped by type, with two check-boxes to select visualizing intra- and/or inter-chain contacts. Contacts can be filtered out by their frequency in the ensemble (only for multi-state structures) and five different color schemes. (**D**) Only for multi-state structures: Conformational Dependent Contact Map grouped by contact type. Each point represents at least one contact between a particular residue and any residues in a specific model or molecular dynamic snapshot.

ing the structure and providing static documentation pages and tutorials. It is implemented using the Angular framework (URL: https://angular.io/) and the Angular Material library (URL: https://material.angular.io/). The latter provides components using the Google Material Design principle and provides the overall style of the RING application. The graph (network) visualization is implemented with the D3 library (URL: https://d3js.org/) and the structure viewer uses an instance of the Mol* Viewer (32).

SERVER DESCRIPTION

Input

The main page features an introduction to RING and an input form, which accepts either a PDB identifier or a structure file. The PDB identifier field features autocomplete functionality and both PDB and mmCIF formats are accepted. As a new feature, RING 3.0 allows the user to upload multi-state files (in PDB and mmCIF format) representing conformational ensembles or MD snapshots as different 'models' for use in a probabilistic network. By default, RING processes all chains and all models (states). Additional options are available for network properties and filtering. More information about how to generate multi-state files from MD trajectories and the meaning of optional fields are provided in the help page. While RING 3.0 in principle has no limitations in the number of models that can be processed, due to restrictions in visualizing large structures, only files of up to 200 MB in size will be accepted by the server. For larger structural ensembles we recommend installing RING 3.0 locally. If the submission to the server succeeds, the user is immediately redirected to the result page which refreshes periodically until the calculation completes. Otherwise an error message is displayed.

Output

The RING output displays a top section with basic information on the executed job (i.e. input file name and parameters, optional job title). It allows the user to download the nodes and edges in text format as well as the full network in JSON format for use in Cytoscape (30) without further processing. Compared to the previous RING version, the plain text format includes an additional column for the model number. The remaining content of the result page changes based on the input type (see Figure 1), which can either be a single- or multi-state structure. In the latter case, network edges represent contact probabilities and an additional panel is displayed.

Single-state structures. RING provides the network as an interactive graph alongside the structure in two separate panels (see Figure 1A, B). When clicking on a graph node or position in the structure, the corresponding elements are highlighted and zoomed in both panels. By default, nodes in both the network and structure are colored by protein chain. A panel on the left side (Figure 1C) allows use of different color schemes (i.e. by amino acid type, residue number, secondary structure, chain or node degree) as well as selecting specific edge types (i.e. H-bond, π–π stack, π–cation, ionic, disulfide, van-der-Waals or interatomic contacts). Both the network and structure visualization panels have additional controls in their top right corner which include the possibility to save a high-resolution image in SVG format.

Multi-state structures. The output for multi-state structures is similar to single-state ones, with the following additions. For structures with multiple models, the graph is replaced by a probabilistic network in which edge thickness is proportional to the contact frequency across models. An additional panel below the graph and structure viewer is added to display a conformational dependent contact map (Figure 1D). This is a heatmap highlighting residues making contacts (rows) in each model (columns) for different interaction types (i.e. H-bond, π–π stack, π–cation, ionic, disulfide, van-der-Waals or interatomic contacts). The panel can be used to visualize contact evolution across models, or over time in case models represent MD snapshots. A high-resolution image in SVG format can be downloaded by clicking on the top right corner as well as all data used to generate the different contact representations, available in CSV format.

Usage example

An NMR structural ensemble (PDB code: 2lpb) of the general control transcription factor Gcn4 central activation domain bound to the mediator coactivator domain 1 of Gal11/med15 contains 13 different conformations (33). Gall11 (chain A) has a four-helix fold with a small hydrophobic cleft. In the bound form, Gcn4 (chain B) partially adopts a helical conformation involving 8 residues, which allows Gcn4 to insert three aromatic/aliphatic residues into the Gal11 cleft (33). The multiple weak interactions between Gcn44–Gal11 contribute to the overall transcriptional activation in yeast and put in evidence a Gal11 recruitment process which is guided by multiple low-affinity interactions (33).

RING generates the residue interaction network for each conformation in the ensemble and calculates the contact frequency by residue (see Figure 2). The contact frequency can be used to identify heterogeneous interactions that dynamically vary across the ensemble, as well as those that are highly conserved. Gal11/Gcn4 is a fuzzy complex (34), showing a highly dynamic protein-protein interface and surprisingly simple, involving only hydrophobic interactions. This allows Gcn4 to bind Gal11 in different conformations mostly involving three residues (W120, L123 and F124), which interact with the hydrophobic cleft of Gal11. These residues, in particular W120 and F124, are identified by RING with the highest number of edges (i.e. degree, at 4.0 and 4.46, respectively). If we observe the contact frequency of the interface residues, there are virtually no residues with inter-chain contact frequency between 50% and 100% (Figure 2). This is characteristic of the fuzzy interactions which are conformational heterogeneous and show ambiguous contact patterns (35`). Restricting visualization in RING of inter-chain contacts to a frequency between 0% and 50%, we can see the conformational heterogeneity of these fuzzy interactions (Figure 2). This behavior is exemplified if we look at the π–π stack inter-chain contacts between Gcn4

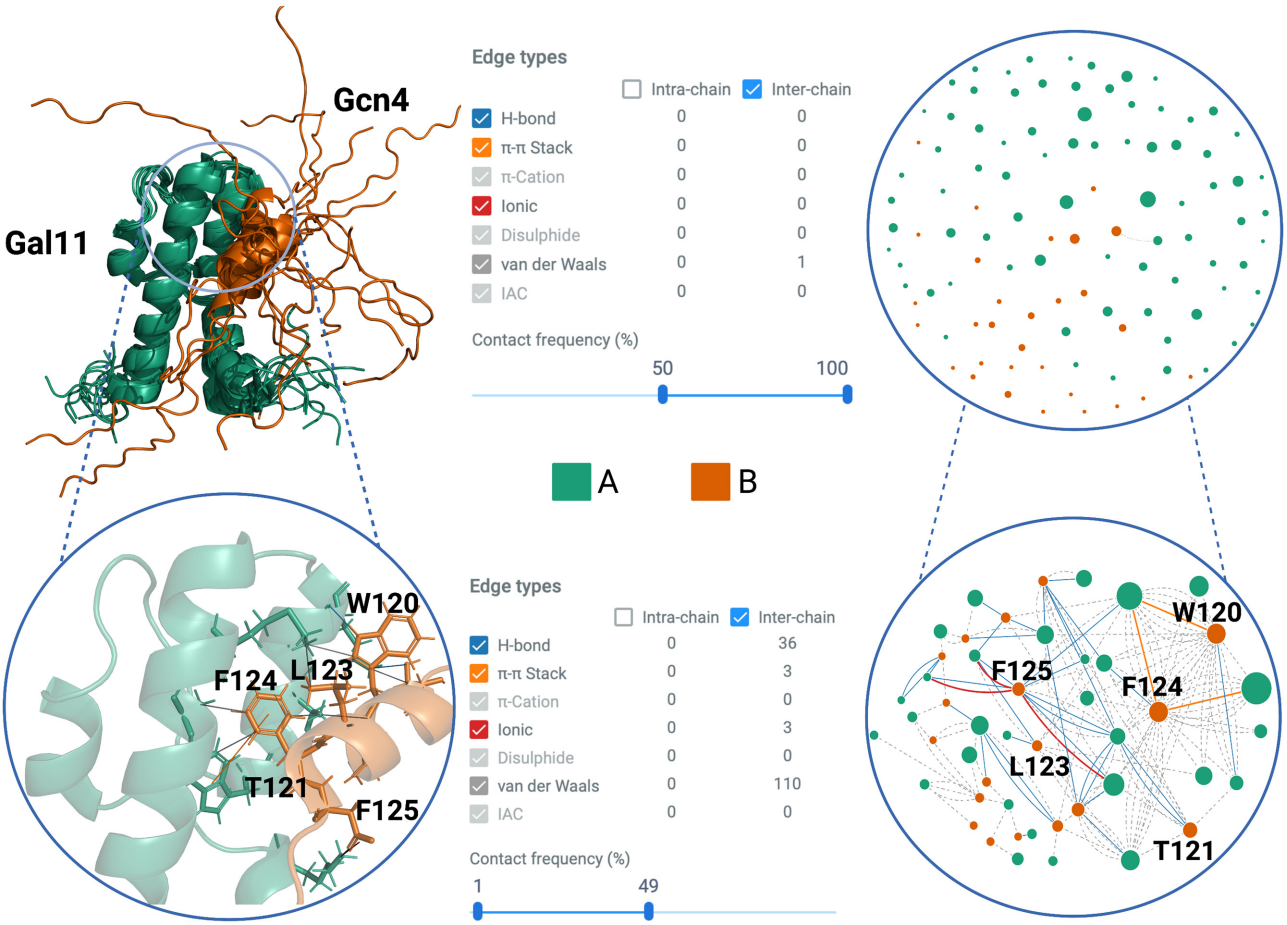

Figure 2. NMR ensemble complex (PDB code: 2LPB) of the mediator coactivator domain 1 of Gal11/med15 (Chain A, green) bound to the central activation domain of Gcn4 (Chain B, orange). The following panels are shown on the top half: Structural ensemble composed of 13 different conformations (left). Summary of inter-chain contacts with a frequency greater than 50% in all models found by RING (center). Resulting inter-contact network with edges and nodes colored by chain and interaction type (right). The following panels are shown in the bottom half: Key Gcn4 residues interactions that dynamically bind Gal11 in one conformation (left). Range of contact frequency in which these inter-chain interactions are found (center). Resulting inter-contact network highlighting edges and nodes involved in the protein-protein interface (right).

residues W120 and F124 and Gal11, which appear in ca. 30% of the conformations. This use case highlights how RING 3.0 can be used to extract meaningful biological information from conformational ensembles.

CONCLUSIONS

RINs are a useful visualization of protein structures as a graph, with residues as nodes and physico-chemical interactions as arcs. RING 3.0 is an extension and improvement of the widely used server for residue interaction network generation, extending the previous server in several ways. A major effort has been focused to improve the underlying software in terms of computational efficiency and management of large molecular complexes. This has allowed the introduction of probabilistic RINs to represent the variability encountered in conformational ensembles and MD simulations. The web interface has been updated to allow the simultaneous exploration of the RIN alongside the structural ensemble for users who are not familiar with Cytoscape. We envisage that RING 3.0 will be useful to more easily identify conformational switches which may be hidden in a large structural ensemble.

DATA AVAILABILITY

RING 3.0 is freely available at: https://ring.biocomputingup.it/.

ACKNOWLEDGEMENTS

This publication is part of a project that has received funding from the European Union's Horizon 2020 research and innovation programme under grant agreement no. 778247 and no. 823886. This work was supported by ELIXIR, the research infrastructure for life-science data. The authors are grateful to members of the BioComputing UP group for insightful discussions.

FUNDING

Italian Ministry of University and Research [PRIN 2017483NH8]; European Union's Horizon 2020 research

and innovation programme [778247, 823886]; ELIXIR Europe. Funding for open access charge: University of Padova.
Conflict of interest statement. None declared.

REFERENCES

1. Dill,K.A. and MacCallum,J.L. (2012) The protein-folding problem, 50 years on. *Science*, **338**, 1042–1046.
2. del Sol,A., Fujihashi,H., Amoros,D. and Nussinov,R. (2006) Residues crucial for maintaining short paths in network communication mediate signaling in proteins. *Mol. Syst. Biol.*, **2**, 2006.0019.
3. del Sol,A. and Carbonell,P. (2007) The modular organization of domain structures: insights into protein-protein binding. *PLoS Comput. Biol.*, **3**, e239.
4. Cheng,T.M.K., Lu,Y.-E., Vendruscolo,M., Lio',P. and Blundell,T.L. (2008) Prediction by graph theoretic measures of structural effects in proteins arising from non-synonymous single nucleotide polymorphisms. *PLoS Comput. Biol.*, **4**, e1000135.
5. Chakrabarty,B., Naganathan,V., Garg,K., Agarwal,Y. and Parekh,N. (2019) NAPS update: network analysis of molecular dynamics data and protein–nucleic acid complexes. *Nucleic Acids Res.*, **47**, W462–W470.
6. Felline,A., Seeber,M. and Fanelli,F. (2020) webPSN v2.0: a webserver to infer fingerprints of structural communication in biomacromolecules. *Nucleic Acids Res.*, **48**, W94–W103.
7 Aydınkal,R.M., Serçinoğlu,O. and Ozbek,P. (2019) ProSNEx: a web-based application for exploration and analysis of protein structures using network formalism. *Nucleic Acids Res.*, **47**, W471–W476.
8. Sheik Amamuddy,O., Glenister,M., Tshabalala,T. and Tastan Bishop,Ö. (2021) MDM-TASK-web: MD-TASK and MODE-TASK web server for analyzing protein dynamics. *Comput. Struct. Biotechnol. J.*, **19**, 5059–5071.
9. Tiberti,M., Invernizzi,G., Lambrughi,M., Inbar,Y., Schreiber,G. and Papaleo,E. (2014) PyInteraph: a framework for the analysis of interaction networks in structural ensembles of proteins. *J. Chem. Inf. Model.*, **54**, 1537–1551.
10. Kayikci,M., Venkatakrishnan,A.J., Scott-Brown,J., Ravarani,C.N.J., Flock,T. and Babu,M.M. (2018) Visualization and analysis of non-covalent contacts using the protein contacts atlas. *Nat. Struct. Mol. Biol.*, **25**, 185–194.
11. Liang,Z., Verkhivker,G.M. and Hu,G. (2020) Integration of network models and evolutionary analysis into high-throughput modeling of protein dynamics and allosteric regulation: theory, tools and applications. *Brief. Bioinform.*, **21**, 815–835.
12. Piovesan,D., Minervini,G. and Tosatto,S.C.E. (2016) The RING 2.0 web server for high quality residue interaction networks. *Nucleic Acids Res.*, **44**, W367–W374.
13. Martin,A.J.M., Vidotto,M., Boscariol,F., Di Domenico,T., Walsh,I. and Tosatto,S.C.E. (2011) RING: networking interacting residues, evolutionary information and energetics in protein structures. *Bioinformatics*, **27**, 2003–2005.
14. Csermely,P. (2008) Creative elements: network-based predictions of active centres in proteins and cellular and social networks. *Trends Biochem. Sci.*, **33**, 569–576.
15. del Sol,A., Fujihashi,H., Amoros,D. and Nussinov,R. (2006) Residue centrality, functionally important residues, and active site shape: analysis of enzyme and non-enzyme families. *Protein Sci. Publ. Protein Soc.*, **15**, 2120–2128.
16. Vendruscolo,M., Paci,E., Dobson,C.M. and Karplus,M. (2001) Three key residues form a critical contact network in a protein folding transition state. *Nature*, **409**, 641–645.
17. Doncheva,N.T., Assenov,Y., Domingues,F.S. and Albrecht,M. (2012) Topological analysis and interactive visualization of biological networks and protein structures. *Nat. Protoc.*, **7**, 670–685.
18. Smith,I.N., Thacker,S., Seyfi,M., Cheng,F. and Eng,C. (2019) Conformational dynamics and allosteric regulation landscapes of germline PTEN mutations associated with autism compared to those associated with cancer. *Am. J. Hum. Genet.*, **104**, 861–878.
19. Piovesan,D., Necci,M., Escobedo,N., Monzon,A.M., Hatos,A., Mičetić,I., Quaglia,F., Paladin,L., Ramasamy,P., Dosztányi,Z. *et al.* (2021) MobiDB: intrinsically disordered proteins in 2021. *Nucleic Acids Res.*, **49**, D361–D367.
20. Mukherjee,S., Erramilli,S.K., Ammirati,M., Alvarez,F.J.D., Fennell,K.F., Purdy,M.D., Skrobek,B.M., Radziwon,K., Coukos,J., Kang,Y. *et al.* (2020) Synthetic antibodies against BRIL as universal fiducial marks for single−particle cryoEM structure determination of membrane proteins. *Nat. Commun.*, **11**, 1598.
21. Bhat,J.Y., Miličić,G., Thieulin-Pardo,G., Bracher,A., Maxwell,A., Ciniawsky,S., Mueller-Cajar,O., Engen,J.R., Hartl,F.U., Wendler,P. *et al.* (2017) Mechanism of Enzyme repair by the AAA+ Chaperone Rubisco activase. *Mol. Cell*, **67**, 744–756.
22. Yan,H., Jiao,H., Liu,Q., Zhang,Z., Xiong,Q., Wang,B.-J., Wang,X., Guo,M., Wang,L.-F., Lan,K. *et al.* (2021) ACE2 receptor usage reveals variation in susceptibility to SARS-CoV and SARS-CoV-2 infection among bat species. *Nat. Ecol. Evol.*, **5**, 600–608.
23. Daskalakis,V. (2018) Protein–protein interactions within photosystem II under photoprotection: the synergy between CP29 minor antenna, subunit s (PsbS) and zeaxanthin at all-atom resolution. *Phys. Chem. Chem. Phys.*, **20**, 11843–11855.
24. Bryant,L., Li,D., Cox,S.G., Marchione,D., Joiner,E.F., Wilson,K., Janssen,K., Lee,P., March,M.E., Nair,D. *et al.* (2020) Histone H3.3 beyond cancer: germline mutations in Histone 3 family 3A and 3B cause a previously unidentified neurodegenerative disorder in 46 patients. *Sci. Adv.*, **6**, eabc9207.
25. Campitelli,P., Modi,T., Kumar,S. and Ozkan,S.B. (2020) The role of conformational dynamics and allostery in modulating protein evolution. *Annu. Rev. Biophys.*, **49**, 267–288.
26. Yu,H. and Dalby,P.A. (2018) Exploiting correlated molecular-dynamics networks to counteract enzyme activity–stability trade-off. *Proc. Natl. Acad. Sci. U.S.A.*, **115**, E12192–E12200.
27. Karamzadeh,R., Karimi-Jafari,M.H., Sharifi-Zarchi,A., Chitsaz,H., Salekdeh,G.H. and Moosavi-Movahedi,A.A. (2017) Machine learning and network analysis of molecular dynamics trajectories reveal two chains of Red/Ox-specific residue interactions in human protein disulfide isomerase. *Sci. Rep.*, **7**, 3666.
28. Hirsh,L., Piovesan,D., Giollo,M., Ferrari,C. and Tosatto,S.C.E. (2015) The victor C++ library for protein representation and advanced manipulation. *Bioinformatics*, **31**, 1138–1140.
29. Westbrook,J.D., Shao,C., Feng,Z., Zhuravleva,M., Velankar,S. and Young,J. (2015) The chemical component dictionary: complete descriptions of constituent molecules in experimentally determined 3D macromolecules in the protein data bank. *Bioinformatics*, **31**, 1274–1278.
30. Shannon,P., Markiel,A., Ozier,O., Baliga,N.S., Wang,J.T., Ramage,D., Amin,N., Schwikowski,B. and Ideker,T. (2003) Cytoscape: a software environment for integrated models of biomolecular interaction networks. *Genome Res.*, **13**, 2498–2504.
31. Morris,J.H., Huang,C.C., Babbitt,P.C. and Ferrin,T.E. (2007) structureViz: linking Cytoscape and UCSF Chimera. *Bioinformatics*, **23**, 2345–2347.
32. Sehnal,D., Bittrich,S., Deshpande,M., Svobodová,R., Berka,K., Bazgier,V., Velankar,S., Burley,S.K., Koča,J. and Rose,A.S. (2021) Mol* viewer: modern web app for 3D visualization and analysis of large biomolecular structures. *Nucleic Acids Res.*, **49**, W431–W437.
33. Brzovic,P.S., Heikaus,C.C., Kisselev,L., Vernon,R., Herbig,E., Pacheco,D., Warfield,L., Littlefield,P., Baker,D., Klevit,R.E. *et al.* (2011) The acidic transcription activator gcn4 binds the mediator subunit gal11/med15 using a simple protein interface forming a fuzzy complex. *Mol. Cell*, **44**, 942–953.
34. Hatos,A., Monzon,A.M., Tosatto,S.C.E., Piovesan,D. and Fuxreiter,M. (2021) FuzDB: a new phase in understanding fuzzy interactions. *Nucleic Acids Res.*, **50**, D509–D517.
35. Monzon,A.M., Piovesan,D. and Fuxreiter,M. (2022) Molecular determinants of selectivity in disordered complexes may shed light on specificity in protein condensates. *Biomolecules*, **12**, 92.